

# Parallel domain decomposition methods for the 3D Cahn-Hilliard equation

Chao Yang<sup>1,2</sup>, Xiao-Chuan Cai<sup>1</sup>, David E. Keyes<sup>3,4</sup>, and Michael Pernice<sup>5</sup>

<sup>1</sup>Dept. of Computer Science, Univ. of Colorado at Boulder, Boulder, CO 80309, USA

<sup>2</sup>Inst. of Software, Chinese Academy of Sciences, Beijing 100190, P. R. China

<sup>3</sup>MCSE Division, King Abdullah Univ. of Science & Technology, Thuwal 23955, Saudi Arabia

<sup>4</sup>Dept. of Applied Physics & Applied Math., Columbia Univ., New York, NY 10027, USA

<sup>5</sup>Idaho National Laboratory, Idaho Falls, ID 83415, USA

E-mail: [chao.yang@colorado.edu](mailto:chao.yang@colorado.edu)

**Abstract.** Domain decomposition methods are studied in a scalable parallel solver for the Cahn-Hilliard equation in 3D. The discretization is based on a stabilized implicit cell-centered finite difference scheme together with an adaptive time-stepping strategy. A Newton-Krylov-Schwarz algorithm is applied to solve the nonlinear system of equations arising at each time step. In the Schwarz preconditioner, we find that low-order homogeneous Neumann boundary conditions on the overlapping subdomains lead to better convergence than do the standard conditions for this fourth-order equation. Numerical tests show that the implicit approach scales well on an IBM Blue Gene/L machine with thousands of processor cores.

## 1. Introduction

The phase-field method is becoming a powerful tool in material sciences and many other fields. A major advantage of the method is that the phase-field variable contains information on the location of all interfaces in the system, without explicitly tracking the evolution of individual interfaces, as in classical sharp-interface methods. Another advantage is that the method, built within the framework of thermodynamics, allows many physical components to be added and treated simultaneously, without destroying the elegance of its mathematical formulation (e.g., [1]). The phase-field method admits a variety of spatial and temporal scales in the system. When the Cahn-Hilliard equation is used to model a spinodal decomposition phenomenon, a rapid phase separation process occurs at early time, followed later by a coarsening process during which the characteristic scale of the system usually grows according to a power law. As a result of the multiscale nature, the partial differential equations arising in many phase-field problems are typically high-order nonlinear parabolic equations containing both diffusive and antidiffusive terms and are often stiff and highly ill-conditioned. Thus special care should be made in designing scalable solvers for this type of problems.

In this paper, we investigate a stabilized, implicit, cell-centered finite difference scheme together with an adaptive time-stepping strategy for the Cahn-Hilliard equation. We apply a Newton-Krylov-Schwarz algorithm to solve the nonlinear system of equations arising at each time step. Low-order homogeneous boundary conditions for the subdomain problems are imposed in

the Schwarz preconditioner. Numerical results on an IBM Blue Gene/L machine with thousands of processor cores are then provided to show the scalability of the overall approach.

## 2. The Cahn-Hilliard equation

In this paper, we consider a binary mixture composed of two species with local concentrations  $c_1(\mathbf{x}, t)$  and  $c_2(\mathbf{x}, t)$ , where  $c_1, c_2 \in [0, 1]$  and  $c_1 + c_2 = 1$ . Here  $(\mathbf{x}, t) \in \Omega \times [0, T] \subset \mathbb{R}^3 \times \mathbb{R}$ . We use  $u(\mathbf{x}, t)$  to represent the concentration difference of the species; that is,  $u = c_1 - c_2 \in [-1, 1]$ . The phase equilibrium is then represented by pure fluids  $u = \pm 1$ .

Phase-field models are usually connected to the thermodynamics through a dissipative minimization of a free energy functional  $E(u)$ . In phase-field modeling, a basic choice for  $E(u)$  is the following Ginzburg-Landau free energy:

$$E(u) = \int_{\Omega} \left( W(u) + \frac{\epsilon^2}{2} |\nabla u|^2 \right) d\mathbf{x}, \quad (1)$$

where  $W(u)$  accounts for the chemical potential functional and  $\epsilon$  is a small positive constant describing the sharpness of the phase interfaces. For a conserved system, the integral of the phase-field variable over space is time-independent, and the equation of motion is

$$\frac{\partial u}{\partial t} - \nabla \cdot m(u) \nabla \frac{\delta E(u)}{\delta u} = 0, \quad (2)$$

where  $m(u) \geq 0$  is the mobility. Substitute the Ginzburg-Landau free energy (1) into the conserved system expression (2), we obtain the following Cahn-Hilliard (CH) equation:

$$\frac{\partial u}{\partial t} + \epsilon^2 \nabla \cdot m(u) \nabla \Delta u - \nabla \cdot m(u) \nabla W'(u) = 0. \quad (3)$$

In the definition of the CH equation, a double-well quartic chemical potential  $W(u) = \frac{1}{4}(1 - u^2)^2$ , together with a constant mobility  $m(u) = 1$ , is widely used in research papers. However, the quartic approximation is inaccurate when the phase quench is deep, that is, the ratio between the critical temperature and the absolute temperature is large; see [2, 3] for more details. A more realistic chemical potential, deduced from the Flory-Huggins model, takes the logarithmic form

$$W(u) = \frac{1}{2} \left[ (1 + u) \ln(1 + u) + (1 - u) \ln(1 - u) - \theta u^2 \right], \quad (4)$$

where  $\theta = 3/2$  represents the quench ratio. When this logarithmic chemical potential is used, a variable mobility  $m(u) = \frac{1}{4}(1 - u^2)$  is often considered for the sake of thermodynamical consistency. It is then easy to verify that the CH equation can be written as

$$\frac{\partial u}{\partial t} + \epsilon^2 \nabla \cdot m(u) \nabla \Delta u + \theta \nabla \cdot m(u) \nabla u - \frac{1}{4} \Delta u = 0. \quad (5)$$

In this paper, for simplicity, we consider only the case in which the computational domain  $\Omega$  is a unit cube, on which we impose periodic boundary conditions or the following Neumann boundary conditions:

$$\frac{\partial u}{\partial \mathbf{n}} = m(u) \frac{\partial \Delta u}{\partial \mathbf{n}} = 0, \quad (6)$$

where  $\mathbf{n}$  is the unit outward normal vector on  $\partial\Omega$ . We remark that the domain decomposition method presented in this paper can be generalized to more complicated domains with other types of boundary conditions.

### 3. Numerical schemes

A cell-centered finite difference scheme on the uniform mesh of  $\Omega$  is employed to spatially discretize the CH equation (5). Then the discretized solution on time level  $t = t_n$  is denoted as  $U^n$ . In this paper, only a first-order time integration scheme is considered; similar analysis can be applied to other higher-order schemes; see [4] for examples.

Since phase-field equations are typically stiff and high-order parabolic partial differential equations, explicit schemes suffer severely from time-step restrictions imposed by the stability limit. Even when a fully implicit or a semi-implicit method is employed, some time-step limit, though not as bad, still exists. For example, it was argued in [3] that the time-step limit for the backward Euler scheme applied to the CH equation is  $\Delta t \leq \mathcal{O}(\epsilon^2)$ . Although it is independent of the mesh size, the restriction is still severe, especially when  $\epsilon$  is small.

Phase-field problems are based on the dissipative minimization of the free energy functional. Time integration schemes should therefore obey a discrete energy law so that the system remains energy stable (e.g., [5, 4]) in the sense that  $\mathcal{E}(U^{n+1}) \leq \mathcal{E}(U^n)$ ,  $n = 1, 2, 3, \dots$ , where  $\mathcal{E}$  is the spatial discretization of the energy functional  $E$ . Because of the nonconvex nature of  $E$ , a certain splitting of  $E$  becomes necessary so that the energy law can be ensured. A key observation first exploited by Eyre [5, 6] reveals that the energy  $E$  admits a splitting, which is not necessarily unique, into a pure convex part and a pure concave part, i.e.,  $E = E_1 + E_2$ . Here the convex energy  $E_1$  has a contractive behavior while the other part  $E_2$  is expansive. The time-step limit can be relaxed, and stabilized schemes can be obtained by treating the expansive term explicitly and the other part implicitly. For example, one such splitting for the CH equation (5) is

$$E_1 = \int_{\Omega} \left( \frac{\epsilon^2}{2} |\nabla u|^2 + \frac{1+u}{2} \ln(1+u) + \frac{1-u}{2} \ln(1-u) \right) d\mathbf{x}, \quad E_2 = - \int_{\Omega} \frac{\theta}{2} u^2 d\mathbf{x}, \quad (7)$$

which leads to a stabilized implicit scheme that we use in this paper.

The evolution of a phase-field problem admits various time scales. For the CH equation, typically, the minimization of the chemical energy results in very fast development in the early stage of the phase separation. Later, in the coarsening process, the dissipation of the interfacial energy is orders of magnitude slower. Therefore, an adaptive time-step control is necessary in the numerical simulation. For a given implicit scheme, an algebraic system

$$F(U, U^n; \Delta t_n) := \frac{U - U^n}{\Delta t_n} + G(U, U^n) = 0 \quad (8)$$

needs to be solved at each time step with step size  $\Delta t_n = t_n - t_{n-1}$ . Here  $G$  is dependent on the spatial discretization and the time integration scheme. The idea of adaptive time-stepping is analogous to the switched evolution/relaxation method in [7] and [8]. More specifically, we start with a relatively safe time-step size  $\Delta t_0 = \mathcal{O}(\epsilon^2)$  and adaptively adjust it by

$$\Delta t_n = \max(1/\alpha, \min(\alpha, \beta)) \Delta t_{n-1}, \quad \beta = \left( \frac{\|G(U^{n-1}, U^{n-1})\|}{\|G(U^n, U^n)\|} \right)^\gamma, \quad n = 1, 2, 3, \dots, \quad (9)$$

where  $\alpha = 1.5$  and  $\gamma = 0.75$  are used to control the adaptivity.

### 4. Scalable domain decomposition method

In the nonlinearly stabilized scheme we use an inexact Newton method to solve the nonlinear system (8) at each time step. The initial guess  $U_{(0)} = U^n$  is set to be the solution of the previous time step. Then the next approximate solution  $U_{(\ell+1)}$  is obtained by

$$U_{(\ell+1)} = U_{(\ell)} + \lambda_\ell S_\ell, \quad \ell = 0, 1, \dots \quad (10)$$

Here  $\lambda_\ell$  is the steplength determined by a linesearch procedure, and  $S_\ell$  is the Newton correction vector. In order to calculate  $S_\ell$  for each Newton iteration, a right-preconditioned linear system

$$J_\ell M^{-1}(MS_\ell) = -F(U_{(\ell)}, U^n; \Delta t_n) \quad (11)$$

is constructed and solved approximately by using a restarted flexible GMRES method. Here the Jacobian matrix

$$J_\ell = \frac{\partial F(U_{(\ell)}, U^n; \Delta t_n)}{\partial U_{(\ell)}} \quad (12)$$

is calculated at the current approximate solution  $U_{(\ell)}$ .

To define the preconditioner  $M^{-1}$ . We first partition  $\Omega$  into  $np$  non-overlapping subdomains  $\Omega_k$ ,  $k = 1, 2, \dots, np$ . An overlapping decomposition can be obtained by extending each subdomain with  $\delta$  mesh layers. Denote the overlapping subdomain as  $\Omega_k^\delta$ . The one-level restricted additive Schwarz (RAS, [9]) preconditioner reads as

$$M^{-1} = \sum_{k=1}^{np} (R_k^0)^T B_k^{-1} R_k^\delta. \quad (13)$$

Here  $R_k^\delta$  and  $(R_k^0)^T$  serve as a restriction operator and an interpolation operator respectively; their detailed definitions can be found in [9].

The subdomain matrix  $B_k$  is crucial to the success of the RAS preconditioner. The key issues here include what boundary conditions should be imposed on the subdomain boundaries and what subdomain solvers are employed. It turns out the usual Neumann boundary condition (6) results in very high iteration numbers. We therefore choose to use the following low-order homogeneous Neumann boundary conditions:

$$u = \frac{\partial u}{\partial \mathbf{n}} = 0, \quad \partial \Omega_k^{\delta + \frac{s}{2}} \setminus \partial \Omega, \quad (14)$$

where  $s$  is the stencil width of the finite difference scheme. For the fourth-order CH equation, the stencil width is  $s = 2$  in the cell-centered finite difference scheme. In order to solve the subdomain problem of  $B_k^{-1}$ , either a sparse LU factorization or a preconditioned iterative method can be employed. When LU is used, the RAS preconditioner is constructed only at the first Newton iteration and is reused for later Newton iterations in the same time step.

## 5. Numerical results

The test case is similar to the ones in [10] and [11] except that  $t$  is scaled by  $2/\epsilon^2$  because of a different, but equivalent, mathematical formulation. Starting from a random initial state  $u_0 = \bar{u} + 0.1 * \text{rand}(-1, 1)$  in  $\Omega = [0, 1]^3$ , interesting steady-state solutions [11] are obtained after long-time integrations. For example, when  $\epsilon^2 = 1/800$  and  $\bar{u} = 0.63$ , a few snapshots of the solutions as well as the time-stepping history are provided in Figure 1, from which we observe that the time-step size is successfully adjusted according to the variation of the solution. In the test, the adaptivity parameter in (9) is fixed to  $\gamma = 0.75$  and  $\Delta t$  is reduced by half if Newton does not converge at a certain time step. Our numerical tests show that the solver failure occurs for less than 10% over all time steps, which is similar to what was experienced in [10].

To investigate the parallel scalability, we solve the same problem on a  $128 \times 128 \times 128$  mesh with different numbers of processor cores ( $np$ ) on an IBM Blue Gene/L supercomputer. The initial time step is  $2.0 \times 10^{-5}$ , and the calculation is stopped at  $t = 0.1$ . The relative stopping conditions for the Newton and GMRES methods are respectively  $1.0 \times 10^{-8}$  and  $1.0 \times 10^{-5}$ . In the preconditioner, we fix the overlapping factor to  $\delta = 2$  and use two different subdomain

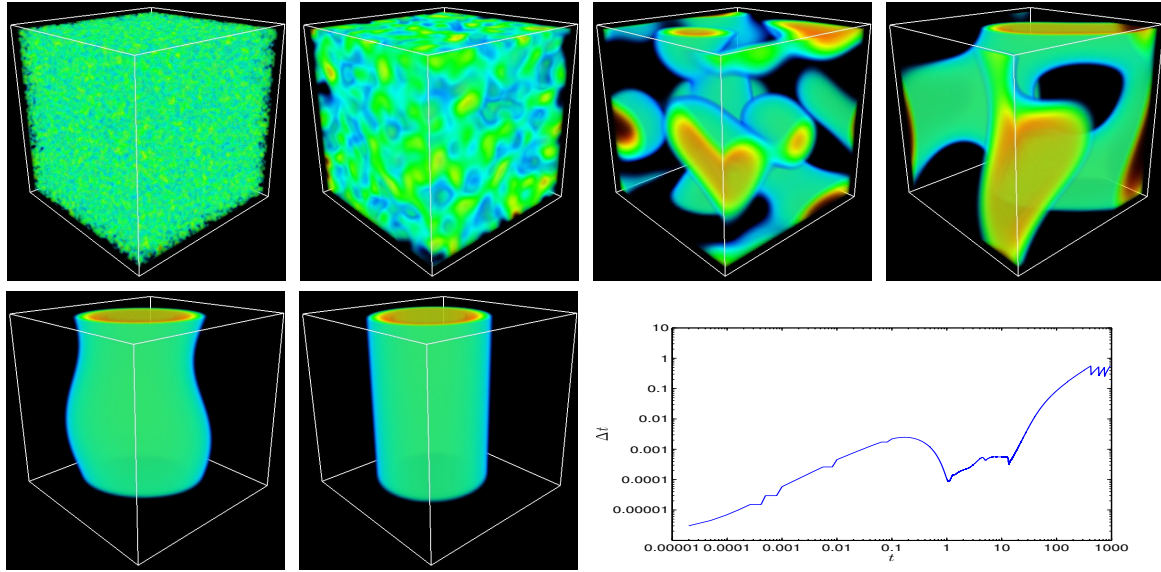


**Figure 1.** Solutions at  $t = 0, 0.0005, 1.2, 4, 16$  and steady state, and the time-stepping history.

solvers, namely, a direct sparse LU factorization and an iterative SSOR preconditioned GMRES method. The total numbers of Newton and GMRES iterations are provided in Table 1, where the total compute times (in seconds) using the two different subdomain solvers are also included. It can be seen that the number of Newton iterations is low and insensitive to  $np$  and the number of GMRES iterations increases slowly as  $np$  doubles. Superlinear speedup is obtained when employing the LU subdomain solver, though the factorization step takes more time than the SSOR preconditioned GMRES does as the size of the subdomain problem becomes larger. Overall, the solver scales well to thousands of processor cores. We remark here that a major advantage of implicit methods over explicit methods is the possibility to achieve acceptable weak scalability [12]. Multilevel Schwarz methods for the CH equation and other phase-field problems are under development and more strong/weak scalability issues will be discussed in a forthcoming paper.

**Table 1.** Scalability results on a  $128 \times 128 \times 128$  mesh.

$np$	Newton	GMRES	Time (LU)	Time (SSOR)
512	45	344	1081.4	427.8
1024	45	373	457.1	276.2
2048	45	396	165.0	156.1
4096	45	410	75.6	88.2

## References

- [1] Millett P C and Tonks M 2011 *Curr. Opin. Solid St. Mater. Sci.* **15** 125–133
- [2] Barrett J W and Blowey J F 1999 *Math. Comp.* **68** 487–517
- [3] Copetti M I M and Elliott C M 1992 *Numer. Math.* **63** 39–65
- [4] Shen J and Yang X 2010 *Discrete Contin. Dyn. Syst. Ser. A* **28** 1669–1691
- [5] Eyre D J 1998 An unconditionally stable one-step scheme for gradient systems (Unpublished article)
- [6] Eyre D J 1998 *Mater. Res. Soc. Sympos. Proc.* **529** 39–46
- [7] Mulder W A and Leer B V 1985 *J. Comput. Phys.* **59** 232–246
- [8] Gropp W D, Kaushik D K, Keyes D E and Smith B *Proc. Supercomputing 2000* IEEE Computer Society
- [9] Cai X-C and Sarkis M 1999 *SIAM J. Sci. Comput.* **21** 792–797
- [10] Gómez H, Calo V M, Bazilevs Y and Hughes T J R 2008 *Comput. Methods Appl. Mech. Engrg.* **197** 4333–4352
- [11] Wodo O and Ganapathysubramanian B 2011 *J. Comput. Phys.* **230** 6037–6060
- [12] Keyes D E, Reynolds D R and Woodward C S 2006 *J. Phys.: Conf. Ser.* **46** 433–442